

A Multifrequency Electron Spin Resonance Study of T4 Lysozyme Dynamics

Jeff P. Barnes,* Zhichun Liang,* Hassane S. Mchaourab,# Jack H. Freed,* and Wayne L. Hubbell[§]

*Baker Laboratory of Chemistry and Chemical Biology, Cornell University, Ithaca, New York 14853-1301; #National Biomedical EPR Center, Medical College of Wisconsin, Milwaukee, Wisconsin 53226; and [§]Jules Stein Eye Institute and Department of Chemistry and Biochemistry, University of California, Los Angeles, California 90095-7008 USA

ABSTRACT Electron spin resonance (ESR) spectroscopy at 250 GHz and 9 GHz is utilized to study the dynamics and local structural ordering of a nitroxide-labeled enzyme, T4 lysozyme (EC 3.2.1.17), in aqueous solution from 10°C to 35°C. Two separate derivatives, labeled at sites 44 and 69, were analyzed. The 250-GHz ESR spectra are well described by a microscopic ordering with macroscopic disordering (MOMD) model, which includes the influence of the tether connecting the probe to the protein. In the faster “time scale” of the 250-GHz ESR experiment, the overall rotational diffusion rate of the enzyme is too slow to significantly affect the spectrum, whereas for the 9-GHz ESR spectra, the overall rotational diffusion must be accounted for in the analysis. This is accomplished by using a slowly relaxing local structure model (SRLS) for the dynamics, wherein the tether motion and the overall motion are both included. In this way a simultaneous fit is successfully obtained for both the 250-GHz and 9-GHz ESR spectra. Two distinct motional/ordering modes of the probe are found for both lysozyme derivatives, indicating that the tether exists in two distinct conformations on the ESR time scale. The probe diffuses more rapidly about an axis perpendicular to its tether, which may result from fluctuations of the peptide backbone at the point of attachment of the spin probe.

INTRODUCTION

The flexibility of proteins is often an integral part of their functioning. It is often required to allow a substrate to bind into a narrow active site; it allows for allosteric control from a distant site on the protein; and for some proteins, the function itself is defined by its conformational cycles (e.g., the contraction of muscle fibers). Inflexible regions are usually a necessary counterpart to this functionality, as beautifully demonstrated in the case of the K⁺ ion channel (Doyle et al., 1998). Many proteins have structures that consist of extended, inflexible regions (denoted as “domains”) connected to one another through relatively flexible regions of the peptide backbone. The dynamics of these proteins in solution might be best described as rigid-body-like rotations of these domains with respect to one another, or alternatively, they might be best described by specifying the amplitude at each site on the peptide backbone of the local fluctuations. It is of interest to understand which description is best for enzymes, because domain dynamics have been hypothesized to play an active role in the catalytic process (Gavish, 1986; Lumry, 1995), in contrast to the current viewpoint (cf. Pauling, 1948). (A typical explanation can be found in Stryer (1988).)

Electron spin resonance (ESR) represents a useful technique for probing protein dynamics. Numerous studies have utilized nitroxide-labeled proteins at ESR frequencies of

9–35 GHz, for which continuous-wave ESR lineshapes are sensitive to motions of nitroxide-labeled proteins in the range of 10⁶ to 10¹⁰ s⁻¹ (Dalton, 1985; Berliner, 1998).

In this study, we extend the ESR analysis of protein motion to include high-field ESR. High-field ESR lineshapes of nitroxide spin probes are sensitive to more rapid reorientational diffusion rates, in the 10¹² s⁻¹ range (Budil et al., 1993), than for 9-GHz ESR studies. The virtue of combining results from two very different frequencies can be appreciated in terms of the fact that the higher-frequency 250-GHz ESR will provide a faster “snapshot” than 9-GHz ESR, so that slower motions will be frozen out on the 250-GHz time scale, but will be important on the 9-GHz time scale. Similarly, faster motions will be completely averaged out on the 9-GHz time scale, but will be important on the 250-GHz time scale. This will clearly be helpful in distinguishing different modes of motion in the complex dynamics of proteins.

Two recent advances have made such measurements feasible. First, techniques have been developed to apply high-field ESR to aqueous samples (Barnes and Freed, 1997). Second, site-directed spin labeling, a method whereby a given sulfhydryl-specific nitroxide reagent is covalently attached to a protein containing a single predetermined cysteine mutation, has been developed (Hubbell et al., 1996). Attachment of the probe MTSSL ((1-oxyl-2,2,5,5-tetramethylpyrrolidine-3-methyl) methanethiosulfonate) at solvent-accessible sites of T4 lysozyme was previously shown not to alter the thermal stability of the enzyme or its enzymatic activity as long as the site is not close to the active site cleft or involved in substrate binding (Mchaourab et al., 1996).

Recent 9-GHz ESR studies of spin-labeled T4 lysozyme in solution (Mchaourab et al., 1996) and of short, α -helical

Received for publication 12 November 1998 and in final form 5 March 1999.

Address reprint requests to Dr. Jack H. Freed, Department of Chemistry, Cornell University, B52 Baker Lab, Ithaca, NY 14853-1301. Tel.: 607-255-3647; Fax: 607-255-0595; E-mail: jhf@msc.cornell.edu.

© 1999 by the Biophysical Society

0006-3495/99/06/3298/09 \$2.00

peptides in solution (Miick et al., 1991; Todd and Millhauser, 1991), as well as 140-GHz ESR studies on several different, but only partly hydrated, spin-labeled proteins (Krinichnyi, 1991; Artyukh et al., 1995) have all reached the conclusion that the reorientational diffusion rates reflected in the ESR lineshapes are correlated with the local motions of the peptide backbone where the probe is attached. They are not strongly correlated with the type of nearest-neighbor amino acid side chains in helical segments (Mchaourab et al., 1996). Unfortunately, it has proved difficult to provide a more quantitative measure of both the internal spin probe dynamics and the protein dynamics from single-frequency ESR studies.

Using the greater information available to the multifrequency ESR approach, we will extend the analysis of the ESR lineshapes to include both the internal dynamics of the spin probe and the overall dynamics of the protein. We will elucidate, through a detailed analysis of both 250-GHz ESR and 9-GHz ESR spectra of spin-labeled T4 lysozyme in solution, the appropriate dynamical model by which to simultaneously analyze the data. It will turn out that the influence of the tether on the spin probe dynamics is reflected in the ESR lineshapes and that the overall diffusive tumbling of T4 lysozyme must be included in the multifrequency ESR analysis. Finally, we seek to understand how these results can be interpreted in terms of the motion of the nitroxide spin probe and the local backbone fluctuations of the protein, and eventually in terms of protein dynamics.

EXPERIMENTAL

Samples consisted of ~ 1 mM spin-labeled mutant T4 lysozyme in a phosphate-buffered solution. The spin-labeled mutants of T4 lysozyme were prepared and purified as previously described (Mchaourab et al., 1996).

For the 9-GHz ESR, 20 μ l of sample was placed in a 0.5 mm i.d. quartz capillary, which was then sealed with wax. For the 250-GHz ESR, 1 μ l of sample was placed in a flat quartz plate sample holder, which has been discussed elsewhere (Barnes and Freed, 1997). The details of the design of the 250-GHz ESR spectrometer at Cornell are discussed by Earle et al. (1996). ESR lineshapes were recorded at 10°C, 22°C, and 35°C, always in that order. Above 45°C, the protein irreversibly precipitates out of solution. The experimental spectra were adjusted to correct for a small admixture of dispersion signal, according to the procedure described by Earle et al. (1993).

The hyperfine (A) tensor and g tensor components and the linewidth (w) tensor components were determined from simulating near-rigid limit ESR spectra. Once determined, they were used as fixed parameters for the fits to the low-viscosity solution ESR data. The near-rigid limit spectra were produced in the following way. Sucrose was added to the T4 lysozyme solution until it was 62% sucrose by weight. This corresponds to a viscosity of 100 cP at room temperature. The 250-GHz and 9-GHz ESR spectra of these samples were then recorded at 10°C.

The near-rigid-limit spectra are shown in Fig. 4. The 9-GHz ESR lineshapes are sensitive to the A tensor parameters, but when the lineshapes are not at the rigid limit, they are less sensitive to the g tensor. The opposite case holds for the 250-GHz ESR lineshapes, except for A_{zz} , which can be accurately determined. Also, the sweep field range for 250-GHz ESR was less precisely known than was the sweep field for 9-GHz ESR. Thus, in fitting these spectra, we first required the value of A_{zz} from the 250-GHz ESR spectra to agree with the 9-GHz ESR fits. This enables us to "fine-tune" the field sweep calibration for the 250-GHz ESR spectra. Second, in

fitting the 250-GHz ESR lineshape, the parameters A_{xx} and A_{yy} were fixed at the values found from the fit to the 9-GHz ESR spectra. Third, in fitting the 9-GHz ESR lineshape, the parameters g_{xx} and g_{yy} were fixed at the values found from the fit to the 250-GHz ESR spectra.

Nonlinear least-squares (NLLS) fits were performed for the 9-GHz and 250-GHz ESR spectra, using the general slow-motional program (Budil et al., 1996). In the near-rigid limit, the spectra are not very sensitive to the precise motional model. Thus, for convenience, axially symmetrical Brownian rotational diffusion was used. The values of R_{\perp} and R_{\parallel} (respectively, the perpendicular and parallel components of the rotational diffusion tensor) were in the range of $1-6 \times 10^6 \text{ s}^{-1}$, consistent with the near-rigid limit. The results are given in Table 1. The uncertainties in the g -tensor and A -tensor components that were obtained directly from these NLLS fits as described by Budil et al. (1996) are comparable to those typically found from NLLS fitting to rigid limit 250 GHz (and 9 GHz) ESR spectra (Budil et al., 1993; Earle et al., 1993, 1997). The small uncertainties in these magnetic tensor parameters are too small to significantly affect the analysis of the motional spectra, as found in previous studies (Budil et al., 1993; Earle et al., 1993, 1997). The g -tensor results show that g_{xx} is slightly lower for site 69 than for site 44, and the A_{zz} values indicate that the unpaired spin density at ^{14}N is lower for site 69 than for site 44. An increase in the polarity of the environment will lower g and raise A (Ondar et al., 1985a). Thus some other mechanism, e.g., a change of the MTSSL ring geometry (Ondar et al., 1985b), is needed to explain the slight variation in the magnetic tensor parameters between the two sites.

Two fitting models were used for the low-viscosity samples, viz. MOMD and SRLS. Briefly, in MOMD we assume that the molecular tether connecting the spin probe to the protein moves in a restricted fashion, such that there is a preferred orientation of the spin probe within the protein molecule. Thus the tether experiences an average torque that tends to align the spin probe into a low free energy conformation. The degree of this constraint is determined in the model by the orientation-dependent potential coefficients, c_{20} and c_{22} . Moreover, the overall rotational motion of the protein is assumed to be too slow on the ESR time scale to affect the spectrum. In the SRLS model, the overall rotational motion of the protein is explicitly included with a rotational diffusion rate, R_0 . When R_0 becomes small enough, the SRLS model reduces to the MOMD model. These two models are discussed at length elsewhere (Polimeno and Freed, 1995).

RESULTS AND DISCUSSION

The 9-GHz and 250-GHz ESR spectra of T4 Lysozyme, spin-labeled at site 44 and at site 69, are shown in Figs. 1 and 2, respectively. In the 250-GHz ESR spectra for site 44,

TABLE 1 The magnetic tensor parameters as determined from the near-rigid limit ESR lineshapes at 9 GHz and 250 GHz, as described in the text

	g_{xx}	g_{yy}^*	A_{xx}	A_{yy}	$A_{zz}^{\#}$	w_{xx}	w_{yy}	w_{zz}
Site 44, 250 GHz ESR	2.00814	2.00597	¶	¶	36.18	4.92	1.81	2.00
Site 44, 9 GHz ESR	§	§	6.18	5.70	36.20	1.30	1.40	1.92
Site 69, 250 GHz ESR	2.00801	2.00586	¶	¶	35.67	4.79	2.42	2.00
Site 69, 9 GHz ESR	§	§	6.42	6.14	35.62	1.43	1.56	1.79

*The estimated relative error is $\pm 5 \times 10^{-6}$, with g_{zz} fixed at 2.00221.

[#]The estimated error is ± 0.2 Gauss.

§Indicates this parameter is fixed at the value found from the 250-GHz ESR spectra.

¶Indicates this parameter is fixed at the value found from the 9-GHz ESR spectra.

^{||}This value was fixed for the fits.

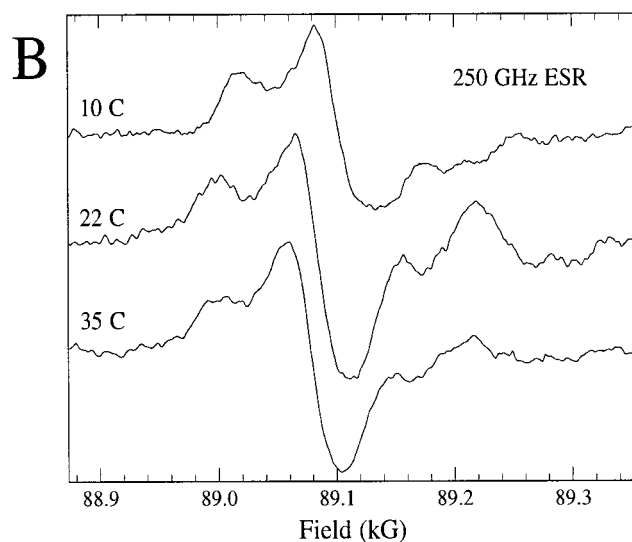
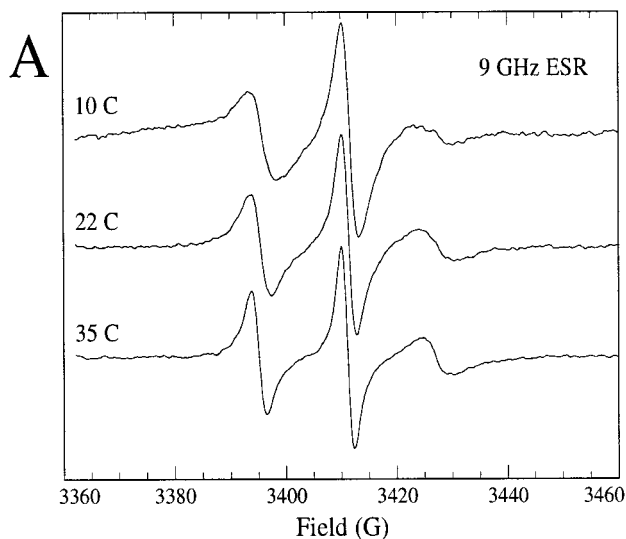


FIGURE 1 ESR spectra (9 GHz and 250 GHz) of T4 lysozyme in solution, spin-labeled at site 44.

a broad, weak line near 89,240 Gauss, or $g = 2.0022$, is present. This slight contaminant obscures some of the lineshape near g_{zz} , but not significantly enough to influence the nonlinear least-squares fits. The contaminant is not observed in the 9-GHz ESR spectra, or in the data from T4 lysozyme labeled at site 69. It could well be present in the 250-GHz spectra for site 44 as a result of the fact that they were averaged over significantly longer periods of time (~ 5 h) than were the other spectra. The ESR spectra at the higher temperatures are motionally narrowed and contain less information on the dynamics and ordering than the 10°C data. Thus we only discuss the analysis of the 10°C data here. We split this section into two parts. In the first, we discuss the dynamical model that should be used to analyze both the 9-GHz and 250-GHz ESR spectra of spin-labeled proteins at 10°C. In the second part, we interpret the parameters from the lineshape analysis in terms of protein dynamics.

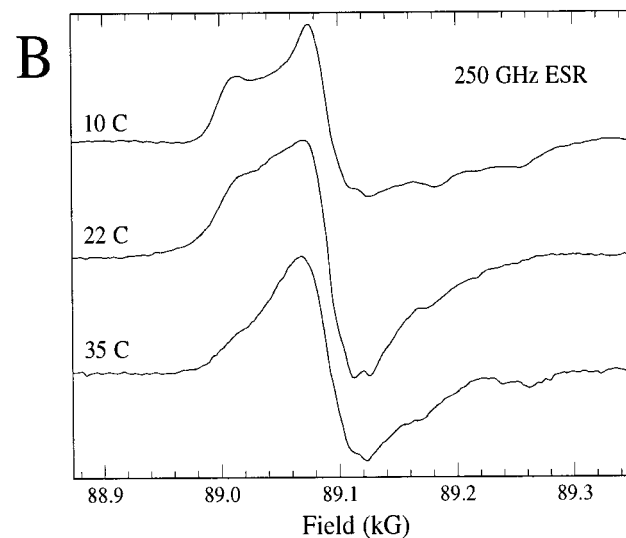
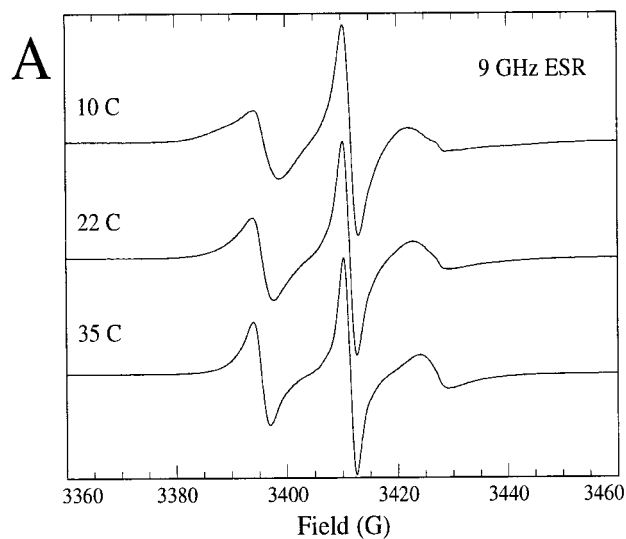


FIGURE 2 ESR spectra (9 GHz and 250 GHz) of T4 lysozyme in solution, spin-labeled at site 69.

Lineshape analysis

The 9-GHz and 250-GHz ESR spectra of T4 Lysozyme in solution at 10°C, spin-labeled at site 44, are shown in Fig. 3. There are two aspects of these spectra that are immediately apparent. First, there are at least two distinct motional/ordering components present. This is demonstrated by the existence of two peaks of greatly differing linewidths at the outer portion of the 9-GHz ESR lineshapes, as indicated by the arrows in Fig. 3 A. The contaminant at $g = 2.0022$ observed in the 250-GHz ESR spectra would be a feature ≤ 20 Gauss in width and centered near 3415 Gauss in the 9-GHz ESR spectra. Thus the contaminant is not likely to alter the outer features in the 9-GHz ESR spectra. Furthermore, we were unable to reproduce all of the features of the 250-GHz ESR lineshape, using only a single component with the fitting models described below (cf. Fig. 3 B).

The second aspect of these lineshapes is that the influence of the molecular tether connecting the probe to lysozyme

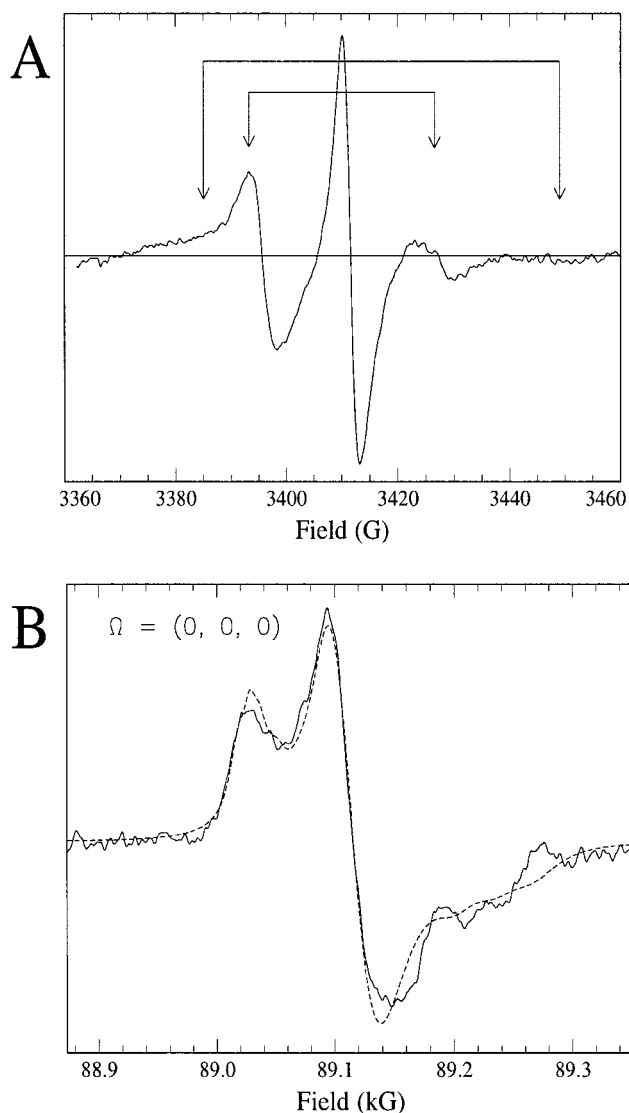


FIGURE 3 Evidence for two components. (A) 9-GHz ESR lineshape of T4 lysozyme at 10°C, labeled at site 44. (B) The 250-GHz ESR lineshape of the same. The arrows for the top spectrum indicate features of the lineshape that suggest a higher-ordered or slower-motional component (*outer arrows*) and a lower-ordered or faster-motional component (*inner arrows*). For the 250-GHz ESR lineshapes, the best MOMD-type single-component fit to the data with no diffusion tilt is shown. It is unable to simultaneously reproduce the sharp peaks at all of the turning points of the g tensor.

can be observed. Specifically, in the 250-GHz ESR spectrum, note that the peaks due to the x and z turning points of the g tensor are contracted toward isotropic g (compare Fig. 3 B with Fig. 4 B). In a Brownian diffusion model, the rotational diffusion rate required to accomplish this contraction would also broaden the peaks to a much greater degree than is observed. Instead, these lineshapes indicate that each spin probe can only reorient within a restricted range of orientations on the 250-GHz ESR time scale, resulting in a “partial averaging” of the lineshape. This constraint results from the stiffness of the tether and the slow reorientational diffusion of lysozyme. If this motion is very slow on the

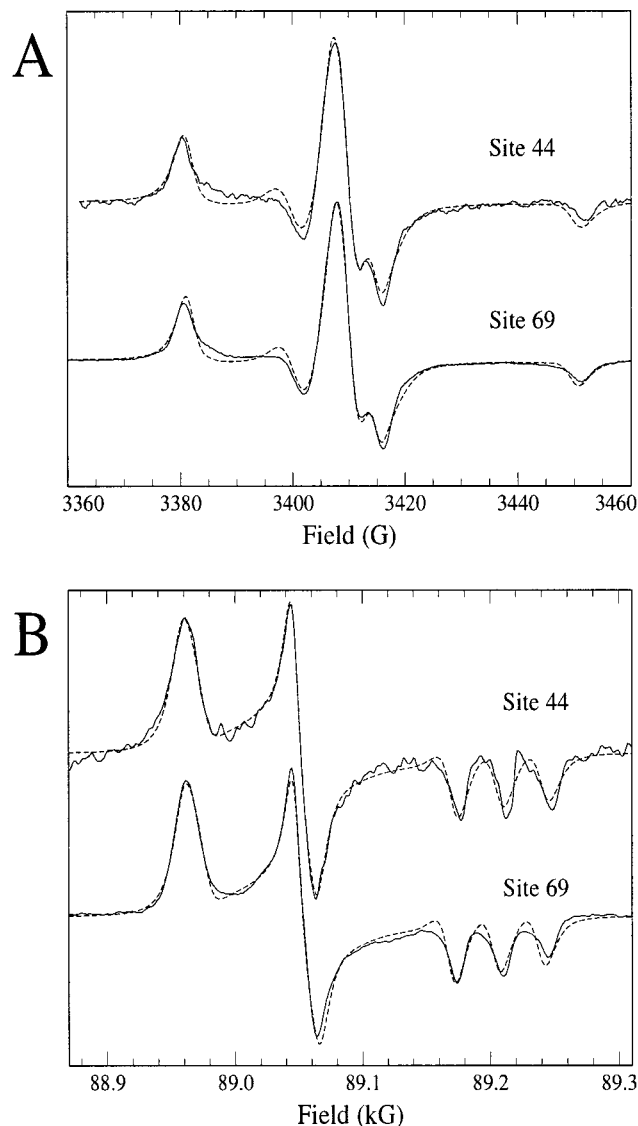


FIGURE 4 (A) 9-GHz ESR spectra and (B) 250-GHz ESR spectra of spin-labeled T4 lysozyme in a sucrose solution of ~ 100 cP viscosity at 10°C, and the near-rigid-limit fits.

250-GHz ESR time scale, then we can model this type of motion by a MOMD lineshape. Briefly, to produce a MOMD lineshape, first an orientation of the tether is specified (i.e., a director frame is defined). An ESR lineshape is calculated for this director frame, within which the spin probe both reorients and is constrained by an orientation-dependent potential. The MOMD lineshape is then the integral of these ESR lineshapes over all tether orientations, because lysozyme reorients in an isotropic fluid.

Shown in Fig. 5 are some possible conformations of the spin label based on the model suggested earlier for the nitroxide side chain on helical surfaces (Mchaourab et al., 1996). The figure conveys the extent of movement of the pyrroline ring allowed by the tether. Observe that rotations about the nitroxide z axis, or perpendicular to the plane of the pyrroline ring, are less hindered than rotations about the

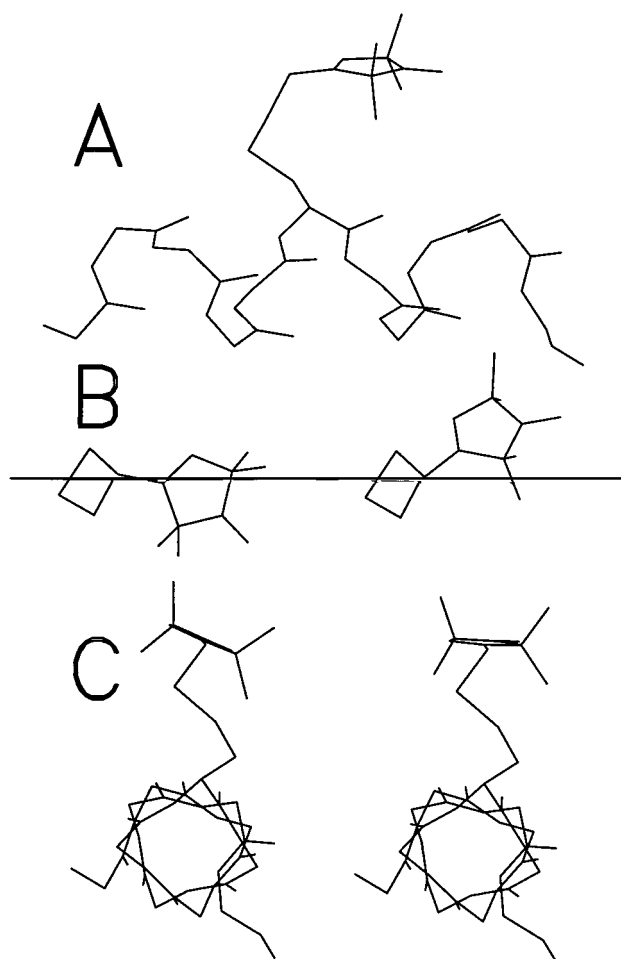


FIGURE 5 Three views, top to bottom, of one conformation of the spin label side chain in a helical sequence (Mchaourab et al., 1996). The views demonstrate the major degrees of rotational freedom allowed by the tether. (A) A view approximately along the nitroxide y axis. (B) Views along the z axis. (C) Views along the x axis. In *B* the α -helix was replaced by a line to better view the pyrroline ring. The tether consists of five bonds, C_{α} - CH_2 - S - S - CH_2 - C (pyrroline). Rotations about the first three tether bonds are highly restricted, apparently because of attractive interactions of the disulfide with main-chain atoms (Mchaourab et al., 1996). The maximum angle of rotation about the last two bonds is determined by steric interactions between the two sulfur atoms and the ring methyl groups. Rotations of up to 120° about the fourth bond but only 20° about the fifth bond are allowed. Rotations about the fourth bond produce motions like those shown in *B*, which is represented by the fit parameter R_z or $R_{||}$, whereas the fifth bond produces motions like those shown in *C*, which are represented by R_x or R_{\perp} .

other two directions (details are given in the figure caption). This suggests that the principal diffusion axis should lie parallel to the nitroxide z axis. This model is appropriate if rotations about the single bond in the tether that produces the motions shown in Fig. 5 *B* dominate the rotational diffusion of the pyrroline ring. It could also be the case that the rotations of all bonds in the tether contribute in an average sense to the rotational diffusion of the spin probe. In that case, the principal diffusion axis should be chosen as the direction from the C_{α} carbon to the carbon atom on the pyrroline ring to which the tether is attached. That situation

is described by a nonzero diffusion tilt of $\Omega_d = (\alpha_d, \beta_d, \gamma_d) = (0^\circ, 25^\circ, 36^\circ)$. We fit to the ESR lineshapes, using either no diffusion tilt or the tilt given above.

The MOMD fits to the 10°C data of the 9-GHz ESR lineshapes and 250-GHz ESR lineshapes with no diffusion tilt are shown in Fig. 6. Those MOMD fits using the diffusion tilt discussed above are shown in Fig. 7. Parameters from these least-squares fits are reported in Table 2 for the 250-GHz ESR lineshapes and in Table 3 for the 9-GHz ESR lineshapes.

Although the fit parameters are sensitive to the presence of diffusion tilt, good fits to the data can be found for either value of Ω_d . However, the parameters for the second component are less well determined, partly because of the broadness of the second component and its overlap with the first component. (Searches for MOMD fits to the 250-GHz ESR data with different signs for the parameter c_{22} for the second component revealed local minima in the parameter space, but with reduced least squares $\geq 20\%$ higher than for the global minimum.) The ambiguity with respect to Ω_d is

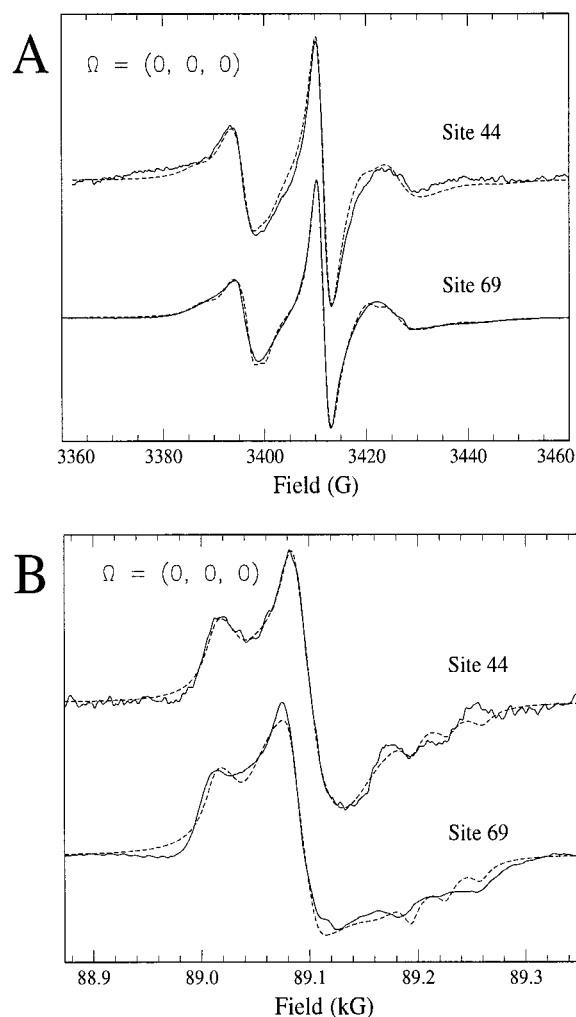


FIGURE 6 (A) 9-GHz ESR spectra and (B) 250-GHz ESR spectra of 1 mM spin-labeled T4 lysozyme at 10°C , and the best MOMD-type fits using no diffusion tilt.

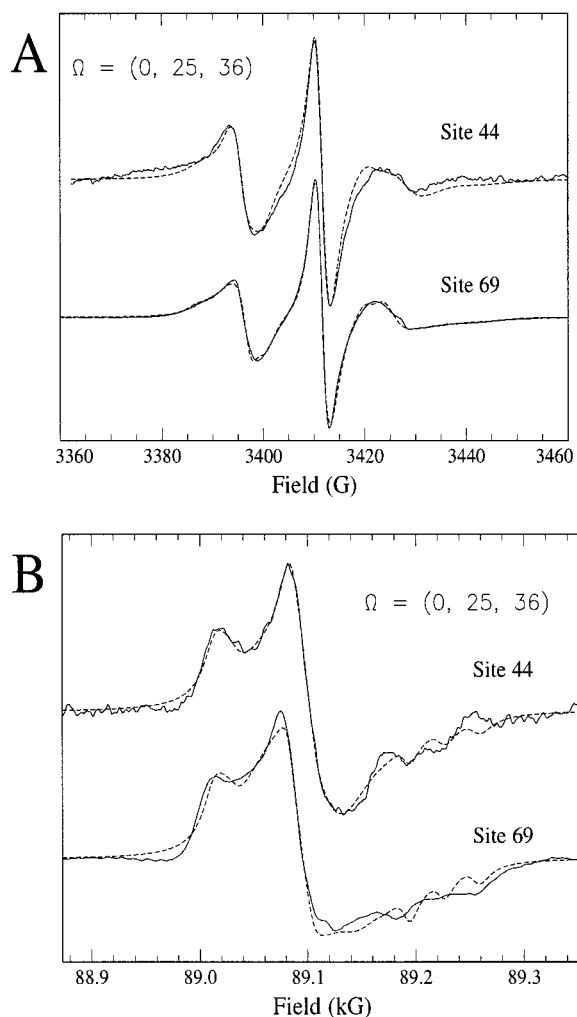


FIGURE 7 (A) 9-GHz ESR spectra and (B) 250-GHz ESR spectra of 1 mM spin-labeled T4 lysozyme at 10°C and the best MOMD-type fits, using a diffusion tilt of $\Omega_d = (0, 25, 36)$.

reflected by the change of the fit parameters with respect to a change in Ω_d . These shifts are thus considered to be an estimate of the errors in determining the parameters. It can be observed that the parameters for the first component are well determined.

The least-squares fits reveal two important facts about the spin label motion that are difficult to discern qualitatively. First, one component has $c_{20} = 4kT$, whereas the other component has a lower ordering potential with $c_{20} = 1.4kT$, with a significant rhombic distortion characterized by non-zero values of c_{22} . Thus the two components are apparently distinguished in large part by the degree of molecular ordering. The second fact about the spin probe motion is that $R_{\perp} > R_{\parallel}$ by nearly a factor of 10. We will return to both of these points in the second half of this section.

We now examine the fits to the 9-GHz ESR lineshapes. Significant discrepancies between the motional/ordering parameters determined by the MOMD fits to the 250-GHz ESR lineshapes (Table 2) and to the 9-GHz ESR lineshapes

(Table 3) can be observed. Although the MOMD fits to the 9-GHz ESR data are good, the parameters are quite different from those found for the 250-GHz ESR lineshapes. However, the two parameter sets can be related through the approximate, empirical relations $c_{20}(9 \text{ GHz}) \approx c_{20}(250 \text{ GHz})/2$, and $R(9 \text{ GHz}) \approx R(250 \text{ GHz})/4$. This is not a result of finding a false minimum in the parameter space: if the 250-GHz ESR fit parameters are fixed in a MOMD fit to the 9-GHz ESR lineshapes, and only the isotropic, homogeneous linewidth is allowed to vary, then the unsatisfactory fit shown in Fig. 8 A results. We offer an explanation for these observations, which will then be supported by quantitative fits shown below.

Lysozyme itself is slowly tumbling in solution with a rotational diffusion rate of $\sim 10^7 \text{ s}^{-1}$ (Brune and Kim, 1993), which is virtually the rigid limit on the 250-GHz ESR time scale. The spin probe, constrained by the tether, will diffuse within the range of orientations allowed it by the tether at a fast enough rate that its effects are observed on the 250-GHz ESR time scale. Thus the rotational diffusion rates refer to the spin probe motion. However, on the slower 9-GHz ESR time scale, both the motion of the spin probe and the overall tumbling motion of the protein will affect the spectrum. Thus the combined spin probe, tether, and protein system will reorient by a more significant amount on the 9-GHz time scale. This will appear to increase the range over which the spin probe can reorient, and thus we expect that the “effective” orientation-dependent potential should be lowered. At the same time, the “effective” rotational diffusion rate will have to be lowered, because it represents a composite of the slower overall rotational rate of the protein and the faster motion of the spin probe.

The above observations imply that a SRLS model is the correct model for fitting the 9-GHz ESR lineshapes (Polimeno and Freed, 1995), because it can simultaneously include both modes of motion. To demonstrate this, a SRLS fit shown in Fig. 8 B, in which only the residual linewidth, and the overall rotational diffusion rate of lysozyme, R_0 , are varied. The rest of the motional/ordering parameters were fixed at the values found from the MOMD fits to the 250-GHz ESR lineshapes (with only a small adjustment of c_{20} allowed for site 69, within its experimental uncertainty). The value found for R_0 is $1.2 \times 10^7 \text{ s}^{-1}$ for site 44 and $1.1 \times 10^7 \text{ s}^{-1}$ for site 69, and $w \approx 1.5$ Gauss for both sites. A comparison between the MOMD and the SRLS fits in Fig. 8 clearly demonstrates the need for the SRLS model for the 9-GHz ESR spectra, if one is to obtain good fits to both 9-GHz and 250-GHz spectra with a single set of fitting parameters.

Thus we see that the multifrequency approach taken here is indispensable for an accurate interpretation of the spectra. This is especially true for the MTSSL spin probe, because the two overlapping components result in a loss of resolution. The 250-GHz ESR lineshapes are significantly more sensitive to the internal dynamics of the spin probe, whereas the 9-GHz ESR lineshapes help to determine the tether and

TABLE 2 Results of fitting to 250-GHz ESR lineshapes alone

MOMD fits to 250 GHz ESR at 10°C										
χ_r^2	Component 1				Component 2					
	R_{\perp}	R_{\parallel}	c_{20}	%	R_x	R_y	$R_z = R_{\parallel}$	c_{20}	c_{22}	%
Site 44, $\Omega = (0, 0, 0)$										
1.16	2×10^8	2×10^7	4.1	42	3×10^8	6×10^8	5×10^6	1.4	-0.9	58
Site 69, $\Omega = (0, 0, 0)$										
113	2×10^8	2×10^7	4.5	35	2×10^9	8×10^7	4×10^8	1.6	0.6	65
Site 44, $\Omega = (0, 25, 36)$										
1.23	2×10^8	2×10^7	4.3	40	4×10^8	4×10^8	2×10^7	0.8	0.0	60
Site 69, $\Omega = (0, 25, 36)$										
125	2×10^8	3×10^7	5.2	34	7×10^8	5×10^7	2×10^8	2.5	-1.7	67

Diffusion rates are in units of s^{-1} , and potentials are in units of kT . The additional linewidth was fixed at 2 Gauss. The errors are estimated to be $\pm 10\%$ for the parameters of component 1, and $\pm 20\%$ for R , and a factor of 2 for the potential coefficients for component 2.

overall lysozyme dynamics. Together, the two well-separated ESR frequencies can provide a unique set of motional/ordering parameters with which to fit the data.

Protein dynamics

The 9-GHz and 250-GHz ESR spectra for sites 44 and 69 differ in quantitative detail but are similar in general features. They are both characterized by two components, and the spin label has similar internal dynamics at the two sites, especially for the first component. However, the percentage of component 1 is lower for site 69 than for site 44, but not by a large amount (34% to 40%, respectively, when diffusion tilt was used).

Most of the fit parameters can be understood to result from the internal dynamics of the spin probe itself. This can be seen from an examination of Fig. 5. Rotations about the fourth bond in the tether are allowed a greater amplitude (Fig. 5 *B*) than rotations about the fifth bond (Fig. 5 *C*) due to steric constraints. For this spin probe, the pyrroline ring is relatively free from steric interactions between nearest-neighbor amino acid side chains (Mchaourab et al., 1996). The restriction of freedom of rotation about the fifth bond or, equivalently, about the nitroxide's x axis, to 20° suggests an orientation-dependent potential with $c_{20} \approx 4kT$ to con-

strain the nitroxide's z axis to remain within 20° of the director axis. In addition, the least-squares fits yield $R_{\perp} \gg R_{\parallel}$. Note that this observation is a consequence of the simultaneous analysis of multiple ESR frequencies. If a nonlinear least-squares analysis is performed on the 9-GHz ESR lineshapes alone, using a MOMD model that ignores the contribution of the protein tumbling, our experience indicates that the fit will produce parameters with $R_{\perp} \ll R_{\parallel}$.

An interesting explanation of the rotational diffusion parameters is that R_{\perp} is selectively increased relative to R_{\parallel} , because of a motion of the peptide backbone to which the spin probe is attached. For example, from Fig. 5 it can be observed that a twisting of the α -helix about its long axis will be equivalent to rotations about the nitroxide's x axis. Such peptide chain motions could be either very local or be due to collective domain dynamics. The fast rate for R_{\perp} ($10^8 s^{-1}$) suggests more localized backbone fluctuations. However, some dynamics simulations do place domain dynamics of lysozyme at these time scales (Gibrat and Go, 1990), although such dynamics are probably best described as diffusive because of strong coupling to the surrounding solvent (Richard et al., 1992; Smith et al., 1990). If this explanation is correct, then multifrequency ESR on spin-labeled proteins is a method by which local peptide backbone fluctuations can be measured using these spin probes.

TABLE 3 9-GHz ESR fits using MOMD-type motion

MOMD fits to 9-GHz ESR at 10°C										
χ_r^2	Component 1				Component 2					
	R_{\perp}	R_{\parallel}	c_{20}	%	R_x	R_y	$R_{\parallel} = R_z$	c_{20}	c_{22}	%
Site 44, $\Omega = (0, 0, 0)$										
25.4	4×10^7	2×10^7	2.22	38	6×10^7	2×10^8	$<10^6$	0.53	0.00	62
Site 69, $\Omega = (0, 0, 0)$										
77.5	6×10^7	8×10^6	2.26	50	1×10^8	1×10^8	$>10^{10}$	0.70	0.01	50
Site 44, $\Omega = (0, 25, 36)$										
26.8	5×10^7	8×10^7	2.05	58	6×10^7	3×10^8	1×10^6	0.47	0.0	42
Site 69, $\Omega = (0, 25, 36)$										
52.7	7×10^7	4×10^5	2.71	32	6×10^7	2×10^8	8×10^6	1.03	-0.94	68

Rotational diffusion rates are in units of s^{-1} , and the potential coefficients are in units of kT . The linewidth tensor was fixed to $w_{xx} = w_{yy} = 0.3$ and $w_{zz} = 0.8$ Gauss. The errors are estimated as being $\pm 10\%$ for the parameters of component 1, and $\pm 20\%$ for R , and a factor of 2 for the potential coefficients, for component 2.

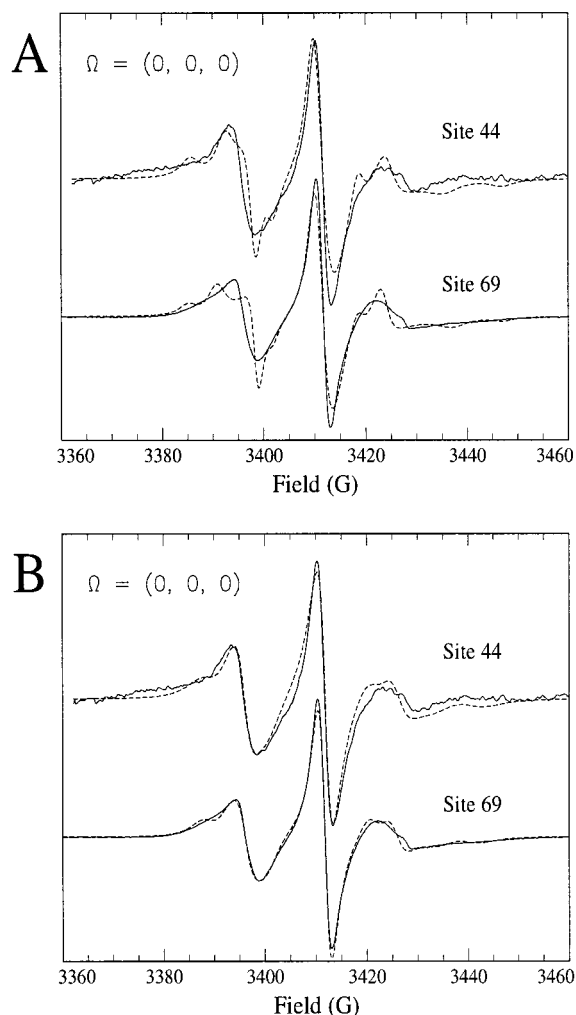


FIGURE 8 A comparison of two fits (---) to the 9-GHz ESR spectra of 1 mM spin-labeled T4 Lysozyme at 10°C (—), but using the parameters found from the MOMD fits to the 250 GHz ESR data. *Top*: The MOMD model. *Bottom*: The SLRS model (for details see text).

CONCLUSIONS

An analysis of multifrequency (9 GHz and 250 GHz) ESR spectra of site-directed, spin-labeled T4 lysozyme at sites 44 and 69 in solution at 10°C, has demonstrated the following: 1) A MOMD motional model is adequate for fitting the 250-GHz ESR lineshapes of this system. The model represents the restricted motion of the tether connected to the protein whose overall motion is too slow to affect the 250-GHz ESR spectrum. 2) For the 9-GHz ESR spectra, a SRLS motional model, which explicitly includes the dynamic effects of the overall rotational motion of the protein, is necessary to achieve consistency with the motional/ordering parameters extracted from the 250-GHz ESR spectra. 3) The disulfide-linked nitroxide side chain used in these studies has two distinct states characterized by different degrees of molecular order. The origin of the two states remains a matter for speculation, but they are likely to correspond to two preferred rotameric states of the side

chain about the C_{α} - C_{β} bond. The nitroxide ring would experience a unique local environment in the rotomers, resulting in different constraints on the diffusive motions. 4) This spin label reorients more rapidly when perpendicular to its tether axis than when parallel to it. This motion cannot be completely explained by the likely internal dynamics of the spin probe tether. The explanation may be that R_{\perp} is measuring fast fluctuations of the peptide backbone at the site to which the spin probe is attached.

This work has clearly demonstrated the advantages of a multifrequency approach. More precise assignments of the details of the dynamics may be expected from studies of spin-labeled mutants at sites yielding a single component, thereby enhancing the spectral resolution, and experiments at additional ESR frequencies that provide more independent data.

This work was supported by National Institutes of Health grants GM25862 (JHF), RR07216 (JHF), and EY05216 (WLH), and the Jules Stein Professorship Endowment (WLH). One of us (JPB) was partially supported by a National Research Service Award GM17174. The computations were performed at the Cornell Theory Center.

REFERENCES

- Artyukh, R. I., G. S. Kachalova, B. A. Samaryanov, and V. P. Timofeev. 1995. Dynamic mobility of the histidine-containing domain in spin-labeled lysozyme. *Mol. Biol.* 29:87–92.
- Barnes, J. P., and J. H. Freed. 1997. Aqueous sample holders for high frequency electron spin resonance. *Rev. Sci. Instrum.* 68:2838–2846.
- Berliner, L. J. 1998. Spin labeling: the next millenium. In *Biological Magnetic Resonance*, Vol. 14. L. J. Berliner, editor. Plenum, New York.
- Brune, D., and S. Kim. 1993. Predicting protein diffusion coefficients. *Proc. Natl. Acad. Sci. USA.* 90:3835–3839.
- Budil, D., K. Earle, and J. H. Freed. 1993. Full determination of the rotational diffusion tensor by electron paramagnetic resonance at 250 GHz. *J. Phys. Chem.* 97:1294–1303.
- Budil, D. E., S. Lee, S. Saxena, and J. H. Freed. 1996. Nonlinear-least-squares analysis of slow-motional EPR spectra in one and two dimensions using a modified Levenberg-Marquardt algorithm. *J. Mag. Res.* A120:155–189.
- Dalton, L. 1985. *EPR and Advanced EPR Studies of Biological Systems*. L. Dalton, editor, Ch. 1. CRC Press, Boca Raton, FL. 1–10.
- Doyle, D., J. Morais, R. Pfuetzner, A. Kuo, J. Gulbis, S. Cohen, B. Chait, and R. MacKinnon. 1998. The structure of the potassium channel: molecular basis of K^{+} conduction and selectivity. *Science.* 280:69–77.
- Earle, K., D. Budil, and J. H. Freed. 1993. 250-GHz EPR of nitroxides in the slow-motional regime: models of rotational diffusion. *J. Phys. Chem.* 97:13289–13297.
- Earle, K., D. Budil, and J. H. Freed. 1996. Millimeter wave electron spin resonance using quasioptical techniques. In *Advances in Magnetic and Optical Resonance*. W. S. Warren, editor, Vol. 19. Academic Press, San Deigo. 253–321.
- Earle, K., J. Moscicki, A. Polimeno, and J. H. Freed. 1997. A 250 GHz ESR study of *o*-terphenyl: dynamic cage effects above T_c . *J. Chem. Phys.* 106:9996–10015.
- Gavish, B. 1986. Molecular dynamics and the transient strain model of enzyme catalysis. In *The Fluctuating Enzyme*. G. R. Welch, editor. Wiley-Interscience, New York.
- Gibrat, J. F., and N. Go. 1990. Normal mode analysis of human lysozyme: study of the relative motion of the two domains and characterization of the harmonic motion. *Proteins Struct. Funct.* 8:258–279.
- Hubbell, W. L., H. S. Mchaourab, C. Altenbach, and M. A. Lietzow. 1996. Watching proteins move using site-directed spin labeling. *Structure.* 4:779–783.

- Krinichnyi, V. I. 1991. Investigation of biological systems by high resolution 2 mm wave band ESR. *J. Biochem. Biophys. Methods.* 23:1–30.
- Lumry, R. 1995. The new paradigm for protein research. In *Protein-Solvent Interactions*. R. B. Gregory, editor. Dekker, New York. 1–136.
- Mchaourab, H. S., M. A. Lietzow, K. Hideg, and W. L. Hubbell. 1996. Motion of spin-labeled side chains in T4 lysozyme. Correlation with protein structure and dynamics. *Biochemistry.* 35:7692–7704.
- Miick, S. M., A. P. Todd, and G. L. Millhauser. 1991. Position-dependent local motions in spin-labeled analogues of a short α helical peptide determined by electron spin resonance. *Biochemistry.* 30:9498–9503.
- Ondar, M. A., O. Ya. Grinberg, A. A. Dubinskii, and Ya. S. Lebedev. 1985a. Study of the effect of the medium on the magnetic resonance parameters of nitroxide radicals by high resolution EPR spectroscopy. *Sov. J. Chem. Phys.* 3:781–792.
- Ondar, M. A., O. Ya. Grinberg, A. A. Dubinskii, A. F. Shestakov, and Ya. S. Lebedev. 1985b. ESR spectroscopy in the two millimeter band and magnetic resonance parameters. *Sov. J. Chem. Phys.* 2:83–92.
- Pauling, L. 1948. Nature of forces between large molecules of biological interest. *Nature.* 161:707–709.
- Polimeno, A., and J. H. Freed. 1995. Slow motional ESR in complex fluids: the slowly relaxing local structure model of solvent cage effects. *J. Phys. Chem.* 99:10995–11006.
- Richard, L., L. Genberg, J. Deak, H. Chiu, and R. J. D. Miller. 1992. Picosecond phase grating spectroscopy of hemoglobin and myoglobin: energetics and dynamics of global protein motion. *Biochemistry.* 31: 10703–10715.
- Smith, J., S. Cusack, B. Tidor, and M. Karplus. 1990. Inelastic neutron scattering analysis of low-frequency motions in proteins: harmonic and damped-harmonic models of bovine pancreatic trypsin inhibitor. *J. Chem. Phys.* 93:2974–2991.
- Stryer, L. 1988. Mechanisms of Enzyme Action. In *Biochemistry*, 3rd Ed. W. H. Freeman, New York. 201–232.
- Todd, A. P., and G. L. Millhauser. 1991. ESR spectra reflect local and global mobility in a short spin-labeled peptide throughout the α helix \rightarrow coil transition. *Biochemistry.* 30:5515–5523.